

Controls on geometry and composition of a levee built by turbidity currents in a straight laboratory channel

D. Mohrig, K.M. Straub & J. Buttles

Department of Earth, Atmospheric and Planetary Sciences, MIT, Cambridge, USA

C. Pirmez

Shell International Exploration and Production, Inc., Houston, USA

ABSTRACT: Experimental results are presented that quantify properties of a channel levee built by depositional turbidity currents. Nine currents of constant initial thickness and composition were released into a pre-existing channel and levee growth on the channel bank was observed. Rates of sediment deposition on the proximal levee, grain size, and taper of levee deposits were all found to be inversely related to local channel depth. These relationships were controlled by 1) the thickness of the depositing current relative to the local channel depth and 2) the vertical profiles of concentration and size for grains suspended within the current. Change in local depth confined more or less current within the channel and determined the fraction of current present at and above the levee-crest elevation where it could act as a sediment source for bank construction. The results are used to develop a simple framework for interpreting submarine levees.

1 INTRODUCTION

Many submarine channels have banks defined by prominent levees. It is generally agreed that these topographic features are built by turbidity currents that spill out of channels and deposit sediment while moving across the overbank surfaces. Unfortunately, direct observations of currents constructing these channel margins are not yet available and specific processes responsible for building submarine levees must be inferred through analyses of their geometry and composition. The laboratory experiment described here resolves, at a reduced scale, many of the interactions between turbidity currents and bottom topography that lead to construction of channel-bounding levees. Analysis of experimental data focuses on establishing the connections between levee thickness, levee taper and composition (grain size). These levee characteristics are in turn related to the following physical properties of the depositing currents: 1) current thickness relative to the local depth of the channel; and 2) vertical profiles of sediment concentration and grain size for the solid particles suspended within the interiors of currents. The experimental results are intended to complement recent quantitative studies of natural submarine levees including those by Skene et al. (2002) and Pirmez and Imran (2003) in order to improve the accuracy with which processes associated with the levee construction can be estimated from the morphology and composition of the levees themselves.

2 EXPERIMENTAL SETUP

The experiment was conducted in a tank 5 m long, 5 m wide and 1.2 m deep (Fig. 1). The initial channel form consisted of 6 concrete segments that were laid end to end, producing a 3 m reach. This channel was trapezoidal in cross-section (Fig. 1). Average width and depth were 0.685 m and 0.050 m, respectively. A map of the initial channel topography is presented as Figure 2A. Each current passed through a momentum reduction box before entering the channel (Fig. 1) so that each flow was a sediment-laden plume driven by buoyancy alone. A 0.4 m deep moat prevented current reflections off of tank sidewalls. The tank remained filled with water throughout the experiment.

The experiment consisted of 9 depositional turbidity currents composed of fresh water plus suspended sediment with an initial volume concentration of 1.5×10^{-2} . The sediment was crushed silica flour with D1, D5, D16, D50, D84, D95, and D99 equal to 1.4 μm , 2.4 μm , 6 μm , 29 μm , 59 μm , 89 μm , and 133 μm , respectively. Each current was pre-mixed in a holding reservoir and introduced to the system via a constant-head tank that ensured a steady entrance discharge throughout each 1 m^3 release of sediment + water. The bulk density for each current as it entered the water-filled tank was 1024 kg/m^3 and current thickness, H , at the channel entrance ($x = 0 \text{ m}$) was set at $9.0 \times 10^{-2} \text{ m}$. Additional initial conditions for the nine currents are summarized in Table 1.

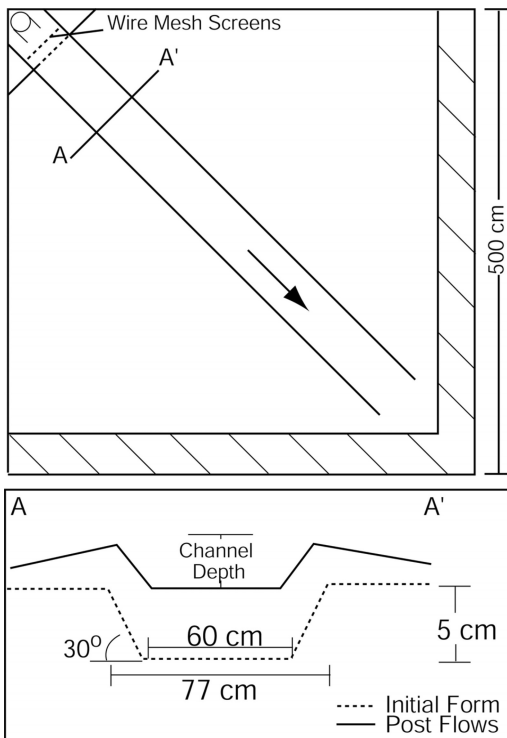


Figure 1. Setup for the straight channel experiment. (top) Plan view of straight channel configuration. Currents enter in top left corner of tank and pass through an excess-momentum diffuser before entering the channel. The moat running along far sidewalls of the tank is marked by a hatched pattern. Piping in the moat removes current from the tank, inhibiting reflections. (bottom) Initial form and an approximate final geometry of a channel cross-section.

The geometric scaling for our experimental system was set at 1/1000. Maximum width, depth and length for the laboratory channel correspond to natural scales of 770 m, 50 m, and 3 km. Additional model-current properties can be compared to natural or prototype systems using three dimensionless parameters; the densimetric Froude number, Fr , the ratio of particle fall velocity to the shear velocity, w_s/u_{*s} , and the Reynolds number, Re . An approximate dynamic similarity between the currents of different scale is ensured by setting $Fr_{(model)} = Fr_{(prototype)}$ (Graf, 1971). This equality yields prototype values for mean streamwise velocity, u , current thickness, H , and current duration of 2.2 m/s, 50 m, and 2.8 hr for current #8. Sediment transporting conditions were mapped between scales by setting $w_s/u_{*s(model)} = w_s/u_{*s(prototype)}$, where $u_*^2 = C_D u^2$, C_D is a bed friction coefficient and w_s was calculated using Dietrich (1982). Values of $C_{D(prototype)} = 2 \times 10^{-3}$ and $C_{D(model)} = 2 \times 10^{-2}$ were used to account for the weak dependence of bed

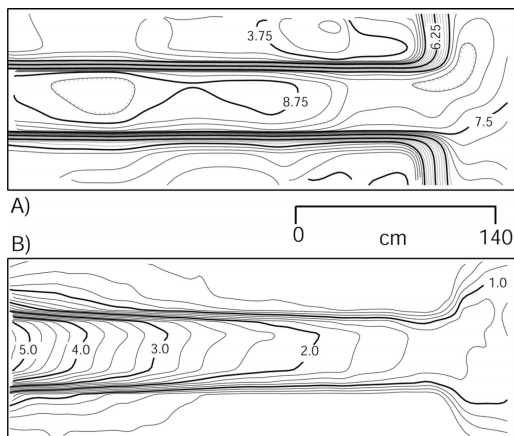


Figure 2. Maps of the 1.27 m \times 3.59 m study area. Flow was from left to right. (A) Initial channel topography. Contour interval is 0.5 cm. (B) Thickness of sediment deposited from the first 8 turbidity currents. Contour interval is 0.5 cm.

Table 1. Characteristics of experimental currents.

Current	u (m/s)	Flow duration (hr)	Fr	Re
1	5.0×10^{-2}	16×10^{-2}	3.4×10^{-1}	4.5×10^3
2	6.0×10^{-2}	16×10^{-2}	4.1×10^{-1}	5.4×10^3
3	5.5×10^{-2}	14×10^{-2}	3.7×10^{-1}	5.0×10^3
4	5.5×10^{-2}	14×10^{-2}	3.7×10^{-1}	5.0×10^3
5	5.0×10^{-2}	14×10^{-2}	3.4×10^{-1}	4.5×10^3
6	7.0×10^{-2}	8.9×10^{-2}	4.7×10^{-1}	6.3×10^3
7	11×10^{-2}	6.8×10^{-2}	7.4×10^{-1}	9.9×10^3
8	7.0×10^{-2}	8.9×10^{-2}	4.7×10^{-1}	6.3×10^3
9	12×10^{-2}	6.9×10^{-2}	8.1×10^{-1}	11×10^3

friction coefficient with turbidity-current scale (Parker et al., 1987; Garcia, 1994). Resulting values for D5, D50, and D95 in the natural system are 7 μ m, 101 μ m, and 434 μ m. $Re_{(model)}$ (Table 1) was always large enough to satisfy the approximate Reynolds similarity for fully turbulent gravity currents proposed by Parsons and Garcia (1998).

An acoustical system was used to produce 5 maps of the channel form; at the beginning of the experiment, after current #1, current #2, current #3, and current #8. The bathymetric measurements were collected with a 1 MHz ultrasonic transducer connected to a pulse/receiver box. Each map was built from 23205 points collected on a 14 \times 14 mm grid and had a vertical resolution of about 100 μ m (Fig. 2). Maps of deposit thickness were produced by differencing successive bathymetric measurements (Fig. 2B).

Average streamwise velocity was measured at the channel entrance using a Sontek ADV (Table 1). A

Sontek PC-ADP was used to measure the streamwise velocity profile at multiple centerline points down the channel. Profile data for current #8 showed that total current thickness remained $9.0 \pm 0.8 \times 10^{-2}$ m halfway down the channel ($x = 1.5$ m) and the velocity maximum was located 2.5×10^{-2} m above the bed.

Following current #9 the tank was drained and samples of the resulting sedimentary deposit were collected for grain-size analysis. The samples were taken from the uppermost deposit and represent deposition associated with final currents. All of the sediment samples were processed using a Horiba LA-300 laser particle-size analyzer.

3 EXPERIMENTAL RESULTS

A primary objective of this experiment was to connect levee development on the channel banks to spatial and temporal variation in the sediment-transport system. One property that varied consistently throughout the experiment was the thickness of currents compared to the local channel depth, h . Currents became increasingly thick relative to the channel topography because initial current thickness was held constant while channel depth systematically decreased via sedimentation. Channel depth decreased through time because sedimentation rates were always greatest inside of the channel, on the channel bed. The cross-section in Figure 3 documents this decrease in channel depth as a function of current number. Figure 3 also documents levee growth with the passage of successive turbidity currents.

All levee data presented here were collected from the bank marked by arrows in Figure 3. Cross-sectional profiles of the levee built by the first 8 currents are shown in Figure 4. These profiles record a consistent change in thickness and taper with streamwise distance. Only the first 0.2 m of the levee was measured, a lateral distance equal to 29% of the channel width. Trends in levee properties are therefore restricted to the most proximal section of the constructional feature.

Streamwise or longitudinal profiles of levee thickness are shown in Figure 5B. These two profiles are associated with the endpoints for the cross-sections in Figure 4. Both profiles (Fig. 5B) show a systematic reduction in levee thickness with distance down the channel. Levee taper was measured perpendicular to the channel direction and calculated by first subtracting the points on one profile from points on the other and then dividing these thickness differences by the lateral distance separating the two profiles. Values for levee taper are shown in Figure 5C and systematically decreased with distance down the channel. It is worth noting that the measured taper would be equal to levee surface slope if the bank of the original channel form had been perfectly flat and horizontal.

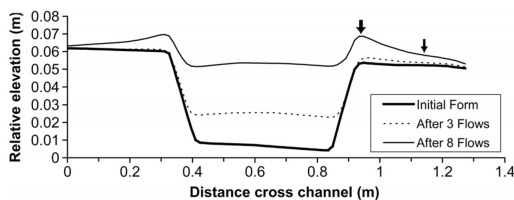


Figure 3. Channel cross section at beginning of experiment, after deposition from 3 currents and after deposition from 8 currents (looking upstream). Section was located 0.35 m from channel entrance. The thick arrow marks the crest of the depositional levee. Grain-size data reported here is from this crest-line profile. The thin arrow marks the position of a second longitudinal profile located 0.2 m from the levee crest-line.

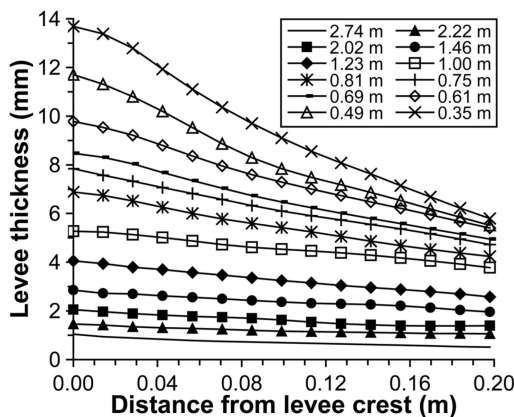


Figure 4. Cross-sectional profiles of the depositional levee at 12 different locations down the channel. Levee thickness and taper decrease with increasing distance from the channel entrance. The longitudinal sections defining the beginning and ending points for all of these levee profiles are marked by the two arrows in Figure 3.

Sediment samples were collected from the uppermost portion of the levee-crest deposit following the release of all nine currents. These samples defined a consistent reduction in the particle size with distance from the channel entrance (Fig. 5D). A smaller number of sediment samples were also collected from the levee along transects running perpendicular to the channel centerline. Size analysis of these samples showed a fining of the levee deposit with distance from its crest line. Unfortunately the number of samples collected was insufficient to accurately resolve this lateral trend in the grain size of the levee.

Sedimentation on the channel bed by the first 8 currents produced a channel form with a local depth that varied with downstream distance (Fig. 5A). This variation in local depth affected levee growth. Data collected from along the channel can be group together

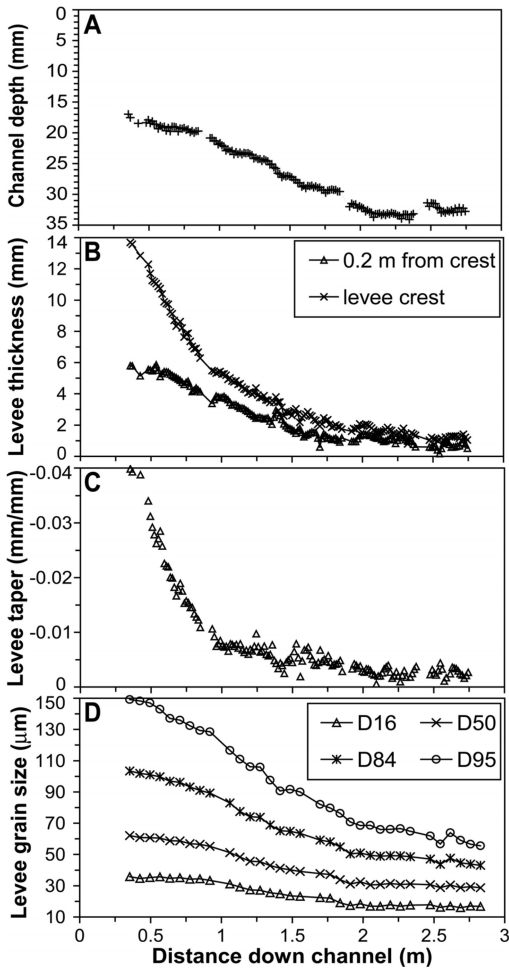


Figure 5. Longitudinal profiles from the channel bed and the levee following sedimentation by 8 currents. (A) Channel depth. Depth equals the elevation difference between the levee crest and the channel bed (see Figure 1). (B) Thickness of levee deposit along the two sections marked by arrows in Figure 3. (C) Lateral taper (thinning) of the proximal levee. Levee taper was calculated by taking the elevation difference between associated points on the two profiles in (B) and dividing this elevation drop by the lateral distance separating the two profiles, 20 mm. (D) Grain size of sediment on the levee crest. D50 is the diameter of the median particle size. D16, D84 and D95 are the representative diameters of the size fractions larger than 16%, 84%, and 95% of the deposited grains, respectively.

to show how sedimentation rate at the levee crest varied as a function of local channel depth. Figure 6 shows that the sedimentation rate at the levee crest was inversely related to local channel depth. Points on the levee crest-line elevated farthest above the bed of the channel had measurably less deposition than

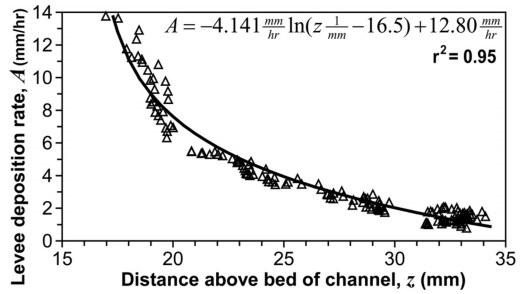


Figure 6. Average sedimentation rate on the studied levee crest as a function of the local channel depth. Graph assembles data from all measured points down the edge of the channel. A best-fit line defining the curve is also shown.

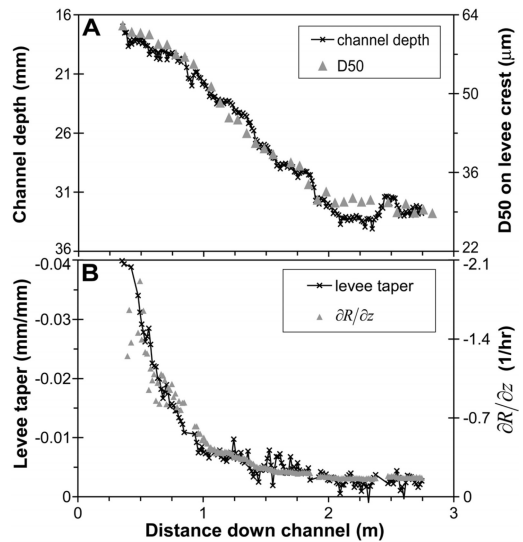


Figure 7. Comparative trends from the experimental channel. (A) Longitudinal variation in channel depth (Fig. 5A) versus median grain size on the levee crest (Fig. 5D). (B) Longitudinal variation in levee taper (Fig. 5C) versus the gradient in sedimentation rate (2) at $z = h$ (Fig. 5A) for all points down the channel.

points where the vertical separation between crest and bed was smaller.

4 INTERPRETATION OF RESULTS

One remarkable property of the experimental system was the correlation found between grain-size on the levee crest-line and downstream change in local channel depth. From inspection of Figure 7A it is clear that the trend for median particle size is a very close match to the longitudinal profile of depth. Particularly compelling is the break in slope present in both

trends at about $x = 2$ m. We envision channel depth controlling levee composition in the following way. The overall size of particles within a turbidity current decreases with distance above its base and a changing local depth acts to confine more or less current within the channel, leaving a finer or coarser-grained portion of current at and higher than the levee crest elevation where it can act as a sediment source for bank construction. This interpretation is supported by the measurements of current thickness collected with the Sontek PC-ADP. These profiles of current velocity record an approximately constant current thickness down the entire length of the channel centerline, suggesting that change in local values of relative turbidity-current thickness, H/h , is primarily related to change in local channel depth.

Deposition rate along the levee crest has already been shown to vary as a function of vertical distance above the local bed of the channel (Fig. 6) so we now turn our attention to processes controlling the magnitude of the levee taper. This taper represents a reduction in deposition rate with distance from the levee crest. Can this spatial change in rate be related simply to a vertical structure within the depositing current? Levee deposition rate, A , in Figure 6 is transformed from a property of the bed into a property of the associated turbidity current through a simple correction for bed porosity. The resulting sedimentation rate, R , for the depositing current is

$$R = (1 - p)A = -2.692 \frac{\text{mm}}{\text{hr}} \ln(z \frac{1}{\text{mm}} - 16.5) + 8.322 \frac{\text{mm}}{\text{hr}} \quad (1)$$

where p is bed porosity = 0.35 and z is vertical distance above the base of the current measured in mm. Equation (1) defines a vertical structure for the representative current and taking the derivative of (1) with respect to z , defines a gradient in sedimentation rate equal to

$$\frac{\partial R}{\partial z} = \frac{-2.692 \frac{1}{\text{hr}}}{z \frac{1}{\text{mm}} - 16.5} \quad (2)$$

Values for (2) are calculated at the levee-crest position, $z = h$, for every point down the channel and plotted in Figure 7B. The measured values of levee taper are also plotted in Figure 7B and it can be seen that taper and $\partial R/\partial z$ are strongly correlated. This correlation is consistent with the lateral taper of the proximal levee being a consequence of the local gradient in sedimentation rate (2) for that fraction of the current moving out onto the bank of the channel. In other words, the vertical structure of the current at the position of the levee crest is translated into a laterally varying deposition rate that builds the levee taper via the lateral advection and settling of suspended particles onto the levee surface. The local sedimentation rate for a strongly depositional turbidity current can be approximated as $R = w_s \varepsilon_s$, where w_s the characteristic settling velocity for the assemblage of depositing particles and ε_s is

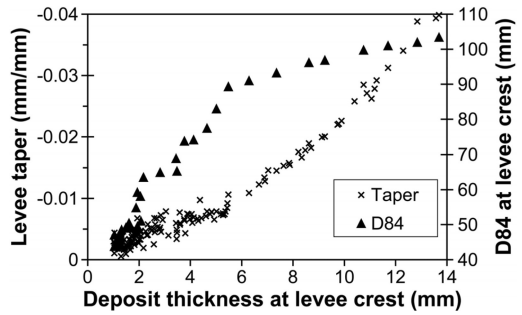


Figure 8. Correlations between levee taper (Fig. 5c), grain size (Fig. 5d) and thickness of the levee-crest deposit.

their volume concentration in the flow directly above the aggrading surface. Levee taper is therefore a product of both the vertical distribution of particle sizes within the supra-channel current and the vertical structure of suspended-sediment concentration within an upper fraction of the flow.

The reduced spatial and temporal scales of the laboratory system allowed for sampling that connected the depositing currents to the developing levee form. Submarine channels are always relatively under-sampled with many components of the system unresolved. Direct measurements of or quantitative estimates for the properties of channel-building turbidity currents are particularly hard to come by. The most abundant data from natural levees are measurements of their geometry. These data may or may not be complimented by boreholes that can provide grain size information at some small number of geographic locations. With these limitations in mind, data from the experimental levee is summarized in Figure 8. This figure highlights the connections between levee thickness, levee taper and levee grain size. The correlations are very clear; 1) variation in levee taper and unit levee thickness is directly related, 2) variation in levee grain-size and unit levee thickness is directly related, and 3) variation in levee taper and levee grain-size is directly related. These results are not surprising, but they form the core of a simple framework for interpreting submarine levees. A measurable change in the thickness of beds composing levee strata should have associated with it a measurable change in the taper of the levee-building beds. If this is observed, a significant change in the grain size of the deposit is predicted, even if borehole confirmation is not available. Additionally, sandier levees should exhibit significantly larger tapers than levees built from muddier deposits.

5 CONCLUSIONS

Analyses of levee deposits associated with submarine channels have been used to estimate the vertical

structure of sediment concentration and grain size for the solid particles suspended within the turbidity currents that built them (Hiscott et al., 1997; Skene et al., 2002; Pirmez and Imran, 2003). The laboratory experiment presented here supports the use of levee deposits in reconstructing properties of depositing flows by documenting the ties between levee thickness, levee taper and levee grain size and the physical properties of the currents. A particularly important flow parameter was the relative thickness of the current. A relatively thick, steep and coarse-grained levee was constructed at locations along the channel where the currents were significantly thicker than the channel was deep and a relatively thin, weakly tapered and fine-grained levee formed where the channel was deeper (Fig. 5). Levee geometry and composition were related to both the absolute concentration and size of the particles suspended in the depositing current at the elevation of the levee crest and to the vertical gradients in concentration and size. The relationships established here need to be tested against geometric and compositional data from natural levees and should be used to refine existing models of channel development that are based on properties of the confining levees.

The levee trends reported here were measured in a straight channel and not affected by any cross-channel variation associated with channel bends. Variability in levee form and composition induced by irregularity in channel plan-form is bound to complicate the connection between properties of the depositing flows and the levees they construct. At the very least, plan-form irregularity increases the number of measurements necessary to resolve any systematic change in levee properties through space or time. The experiment here indicates that geometric and compositional trends for a levee are best defined close to the levee crest. We suggest that future studies of levees on submarine channels should focus on that portion of the form within one channel width of the channel

sidewalls. This proximal section of levees has been under sampled (Pirmez and Imran, 2003) and an emphasis here should provide information that can be used to significantly improve our understanding of submarine channel evolution.

ACKNOWLEDGEMENTS

Support for our research was provided by Shell International Exploration and Production, Inc. and the STC Program of the National Science Foundation under Agreement Number EAR-0120914.

REFERENCES

- Dietrich, W.E. 1982. Settling velocity of natural particles. *Water Resources Research* 18(6): 1615–1626.
- Garcia, M.H. 2004. Depositional turbidity currents laden with poorly sorted sediment. *Journal of Hydraulic Engineering* 120: 1240–1263.
- Graf, W.H. 1971. *Hydraulics of sediment transport*. New York: McGraw-Hill.
- Hiscott, R.N., Hall, F.R. & Pirmez, C. 1997. Turbidity current overspill from the Amazon Channel: texture of the silt/sand load, paleoflow from anisotropy of magnetic susceptibility, and implications for flow processes. In R.D. Flood, D.J.W. Piper, A. Klaus and L.C. Peterson (eds.), *Proceedings of the ODP Sci. Results 155*. College Station: Ocean Drilling Program. 53–78.
- Parker, G., Garcia, M., Fukushima, Y. & Yu, W. 1987. Experiments on turbidity currents over an erodible bed. *Journal of Hydraulic Research* 25: 123–147.
- Pirmez, C. & Imran, J. 2003. Reconstruction of turbidity currents in Amazon Channel. *Marine and Petroleum Geology* 20: 823–849.
- Skene, K., Piper, D. & Hill, P. 2002. Quantitative analysis of variations in depositional sequence thickness from submarine channel levees. *Sedimentology* 49: 1411–1430.